frontiers | Frontiers in Marine Science

TYPE Original Research
PUBLISHED 28 January 2025
DOI 10.3389/fmars.2024.1525195

OPEN ACCESS

EDITED BY
Yang Yang,
Nanjing Normal University, China

REVIEWED BY
Xin Shan,
Ministry of Natural Resources, China
Shan Liu,
Sun Yat-sen University, China

*CORRESPONDENCE
Bing Deng
dengbing@sklec.ecnu.edu.cn

RECEIVED 08 November 2024
ACCEPTED 18 December 2024
PUBLISHED 28 January 2025

CITATION
Deng B and Chen J (2025) Characteristics of seismic strata in the southeast Zhoushan Archipelago (East China Sea) with emphasis on shallow gas. *Front. Mar. Sci.* 11:1525195. doi: 10.3389/fmars.2024.1525195

Characteristics of seismic strata in the southeast Zhoushan Archipelago (East China Sea) with emphasis on shallow gas

Bing Deng[1*] and Junbing Chen[2]

[1]State Key Laboratory of Estuarine and Coastal Research, East China Normal University, Shanghai, China, [2]Zhejiang Institute of Hydrogeology and Engineering Geology, Ningbo, China

Based on high-resolution sub-bottom seismic profiles collected on the coast of the Zhoushan Archipelago in the East China Sea, the distribution and characteristics of shallow gas have been analyzed. The strata in the area were divided into three geological units: Holocene fine-grained neritic facies muddy strata, Late-Pleistocene coarse-grained fluvial or lacustrine facies sandy strata, and bedrock. The presence of shallow gas was evidenced by various acoustic indicators, including acoustic blanking, enhanced reflections, gas chimneys, bright spots, and small mounds. Shallow gas accumulations are observed through the Lower and Upper Holocene strata, presumably related to the degradation of organic matter buried in the Holocene deposits and sealed by soft muddy deposits. The presence of ultra-shallow gas-charged sediment sealed by fine-grained muddy sediment in coastal areas with frequent human disturbance suggests a high potential for sediment instability. Moreover, frequent upward gas migration signatures were found in the study area. These gas migration features mainly occur in nearshore areas where tidal disturbance and human activities are both active. We therefore deduced that the deduction of sediment above probably decreased the pressure, thereby resulting in increased upward migration. The presence of active shallow gas within thin, soft muddy strata, along with the strong tidal turbulence and human activities, indicates that the seafloor of the study area is vulnerable to sediment erosion, and shallow gas is easily released, posing a potential danger to the stability of marine engineering foundations. Since the Changjiang sediment supply has been decreasing over the past decades, it will inevitably lead to corresponding morphological adjustments in the study area, such as seafloor erosion. To what extent coastal erosion will release the buried shallow gas and lead to unpredictable consequences is worthy of our sustained attention.

KEYWORDS

shallow gas, holocene, sub-bottom profiles, acoustic characteristics, strata stability

1 Introduction

Shallow gas is defined as any type of gas buried in loose sediments. It predominantly consists of CH_4, CO_2 H_2S, and/or other gas phases (Davis, 1992). The gas may exist either dissolved or as free discharge within the pore spaces of sediments and strata (Duan and Mao, 2006; Mazumdar et al., 2009). Anaerobic bacterial methanogenesis of buried organic matter is a primary mechanism for generating shallow gas in loose sediments (Scott et al., 1994; Reeburgh, 2007). Shallow gas has been reported in lacustrine and coastal environments (Emeis et al., 2004; Mazumdar et al., 2009; Lin et al., 2010; Dondurur et al., 2011; Sun et al., 2012; Lazar et al., 2012; Schatter et al., 2012; Cukur et al., 2013), particularly in deltaic environments characterized by high rates of sediment accumulation and organic matter burial (Orange et al., 2005; Deng et al., 2006; Allision et al., 2010; Lin et al., 2015). Shallow gas can be destructive or even hazardous to coastal engineering. Gas-charged sediment can substantially change geotechnical properties and seabed stability by reducing the shear strength of surface sediments (Whelan et al., 1977; Ye et al., 2003). Moreover, gas blow-out hazards under overpressure conditions have been frequently reported (Ye et al., 2003; Zhou et al., 2016). Therefore, understanding the presence and distribution of shallow gas in sediments is of great importance for offshore construction safety.

Seismic reflection methods are particularly effective for identifying, characterizing, and mapping the distribution of gas accumulations (Davis, 1992; Cukur et al., 2013). When present in loose sediments and strata, even at low concentrations (~ 0.1% free gas content), free gas can substantially decrease compressional-wave velocity, increase compressional-wave attenuation, enhance sound scattering (Wilkens and Richardson, 1998; Missiaen et al., 2002). These effects result in acoustic anomalies in seismic data, which can be used to identify the shallow gas in sediments and strata (Judd and Hovland, 1992, 2007; Taylor, 1992; Hustoft et al., 2010; Dondurur et al., 2011).

The inner shelf of the East China Sea (ECS) is mainly covered by Changjiang-derived mud, including the proximal and distal subaqueous deltas of the Changjiang. The circulation system plays an important role in the formation of inner-shelf mud areas (Guo et al., 2000). Sediment transport and deposition are dominated by the southward-flowing China Coastal Current and exhibit a pattern of summer deposition and winter transport (Qin and Zheng,1982; Guan, 1982; Li et al., 2005; Gao, 2010). These findings were all based on analyses of seafloor surficial sediment analyses (Shepard et al., 1949; Qin and Zheng, 1982). The use of high-resolution seismic profiles and isotopic dating techniques has expanced knowledge of the internal architecture, sediment budget flux, and development history of coastal mud wedge (Chen et al., 2004; Liu and Milliman, 2004, 2007; Yang and Chen, 2007; Xu et al., 2012; Xu, 2013; Wang et al., 2015). Using eight elongated inner-shelf mud wedge seismic profiles, Liu et al. (2006, 2007) reported northern (on the modern Changjiang delta) and southern (at ~ 27.5° N) depocenters of the mud wedge, discussed the development history of the Changjiang deposit, and proposed a preliminary sediment budget. Xu et al. (2012) subsequently reported that Changjiang sediment accumulation showed two periods of high accumulation rates and one period of low accumulation rates, based on Chirp seismic and AMS radiocarbon dating data. Meanwhile, the presence of shallow gas in seismic profiles has been widely reported (Ye et al., 2003; Chen et al., 2004; Liu et al., 2007).

The Zhoushan mud area is located to the west of the distal Changjiang subaqueous delta (Figure 1A). It is not only the pathway to the south for the Changjiang Dilutes Water but also the main channel for water exchange between the Changjiang delta, Hangzhou Bay, and the East China Sea (Liu et al., 2007; Hu et al., 2009). The Zhoushan sea bottom is characterized by rough topography, including steep rock cliffs, subtidal platforms, and deep troughs (Dong et al., 2018). Although the suspended sediment concentration is high (Hu et al., 2009), the characteristics of sediments and modern sedimentation rate still change significantly with water depth and seabed topography due to the complicated hydrodynamic environment (Xia et al.,2004; Wang et al., 2004; Jiang, 2001). Moreover, despite studies showing that the sediment in the Zhoushan mud area is mainly derived from the Changjiang (Xia et al., 2004; Zhou et al., 2009), it is still not clear whether the dominant role of the study area is as a passage or a trap for sediments from the Changjiang River.

Moreover, the Changjiang sediment flux to the estuary has continued to decline over the past decades due to intensifying human activities in the river basin, especially after the completion of the Three Gorges Dam (TGM) (Yang et al., 2004, 2006, 2011). The decrease in sediment discharge has lead to a significant reduction in the sedimentation rate in the adjacent sedimentary environments, causing the accretional coast to turn into erosion (Yang et al., 2006, 2011; Zheng et al., 2011). To what extent the Zhoushan Archipelago will respond to such a dramatic decrease in sediment supply in the future is also unclear. Moreover, as it is rich in deep port shoreline resources, more intensive engineering activities are either being planned or are already in implementation in the Zhoushan Archipelago to meet the increasing demands for transportation capability in East China. However, little attention has been given to the sedimentary strata and their influence on seabed stability, especially regarding sediment erodibility and the potential hazardous geological features in the study area.

We collected high-resolution sub-bottom seismic data along with published lithology and radiocarbon dates of cores. The objectives of this study are as follows: (1) to delineate sequence boundaries and examine the internal structure and depositional history; (2) to identify acoustic anomalies associated with shallow gas accumulation and analyze the relationship between the distribution of shallow gas and the stratigraphic structure; and (3) to discuss strata stability in relation to shallow gas and the risks of coastal erosion.

2 Datasets and methods

Sub-bottom seismic data in the study area were collected onboard in July 2013 using an EdgeTech 512i Chirp sonar

(EdgeTech Instruments, West Wareham, MA, USA). Profile A and profile B were collected onboard in August 2012 and July 2013, respectively. The working frequency was 0.5–7.2 kHz. The data were postprocessed using an acoustic velocity of 1,500 m/s to calculate depth and sediment thickness, as recommended by Liu et al. (2006). Penetration into the sediments reached up to 50 m, and the vertical resolution was 0.2 m. The data collected in this study comprise 136 km, including 12 main lines and 19 secondary lines (Figure 1B), at a ship speed of 2–3 knots. A DGPS-DSM132 Receiver was installed and connected to the profiler for positioning during the survey. The Discover SB 3200-XS software was simultaneously used for acoustic data interpretation and mapping. Three units and shallow gas were recognized based on their distinct acoustic feature. The recorded digital data, including seabed tracking and identification of the reflection interface, were processed using Triton Perspective software. Using these digital data, we constructed isopach maps of stratigraphic units and the shallow gas front in Golden Surfer software (Figure 2). The stratigraphic structure and geological evolution were mainly based on the acoustic profiles A and B, along with four boreholes selectively chosen from published references.

3 Regional setting

3.1 Study area

The study area, located on the coast of Shenjiamen, Zhoushan Island includes the coast of Zhujiajian Island, Dengbu Island, and Putuo Island at a longitude of 122.2° to 122.4°E and latitude of 29.85° to 30.05°N, is in the south-eastern part of Zhoushan Archipelago sea area (Figure 1B). It is located to the southeast of the Changjiang River Mouth, at the outer edge of Hangzhou Bay and connect with offshore of ECS (Figure 1A). Mainly affected by the southward-flowing East China Sea Coastal Currents (ECSCC) carrying Changjiang Dilutes Water (CDW) and the northward Taiwan Warm Current (TWC) (Lee and Chao, 2003). The tide is typically semi-diurnal in the study area, with a mean tidal range of 2.4 m and a maximum range of 4.7 m (Luo et al., 2014). The average tidal current speeds are 0.82 for spring tide and 0.44 m/s for tide, with a maximum of 1.73 m/s (Dong et al., 2018). The suspended sediment concentrations range from 0.01 to 0.90 kg/m^3 (Dong et al., 2018). The influence of the wave is weak due to the shielding effect of the island.

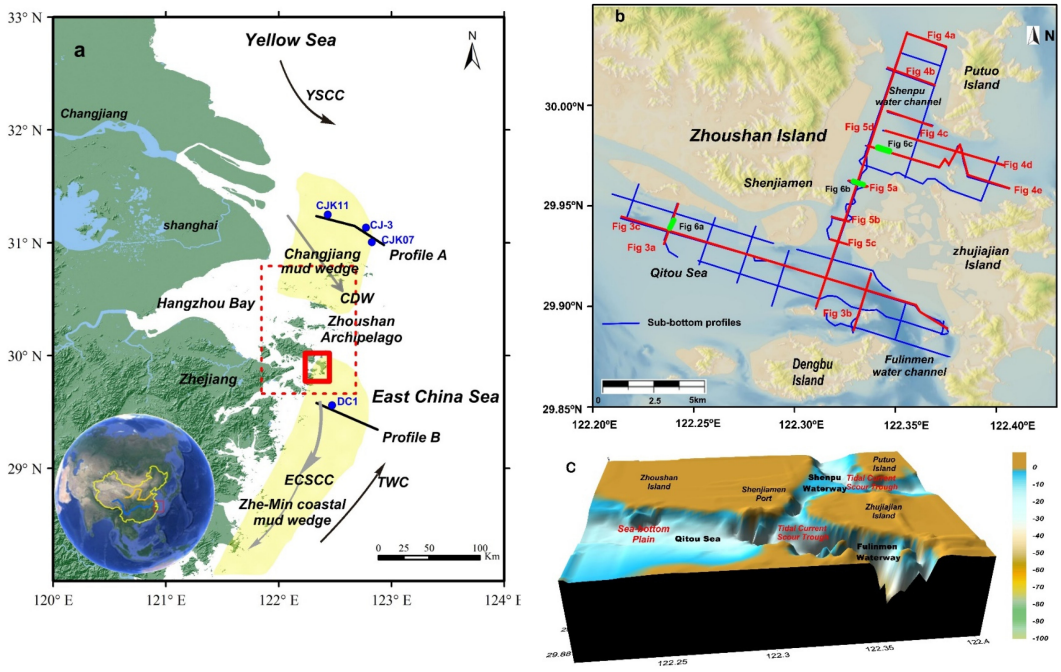

FIGURE 1
The study area and locations of sub-bottom profiles. **(A)** The East China Sea inner shelf and Changjiang sediment dispersal systems. Yellow-shaded areas represent the East China Sea coastal mud wedge, comprising the northern Changjiang submerged deltaic mud wedge and the southern Zhe-Min coastal mud wedge. The red dashed rectangle marks the Zhoushan Archipelago, located between the northern Changjiang depocenter and the southern Zhe-Min coastal depocenter. The red solid rectangle indicates the study area, located in the southeast Zhoushan Archipelago. Blue dots indicate boreholes (Qin et al., 1987; Huang et al., 1996; Xu et al., 2016). Arrows represent major currents in the East China Sea and the Yellow Sea, including the Taiwan Warm Current (TWC), the Changjiang Diluted Water (CDW), the East China Sea Coastal Current (ECSCC), and theYellow Sea Coastal Current (YSCC). Black segments mark sub-bottom acoustic profiles, with profile A collected in 2012 and profile B collected in 2013. **(B)** Sub-bottom profiles collected in 2013 (blue and red lines). Red segments, marked with figure numbers, indicate the locations of seismic profiles shown in Figures 3–5. Thick green lines, marked with figure numbers, indicate the locations of seismic profiles shown in Figure 6. **(C)** Bathymetry of the study area, subdivided into two morphologic units: the tidal current scour trough and the sea-bottom plain. Bathymetry is acquired and processed using Triton Perspective software, with the land portion interpolated to > 0 m. The map was made using Surfer 11 Golden Software.

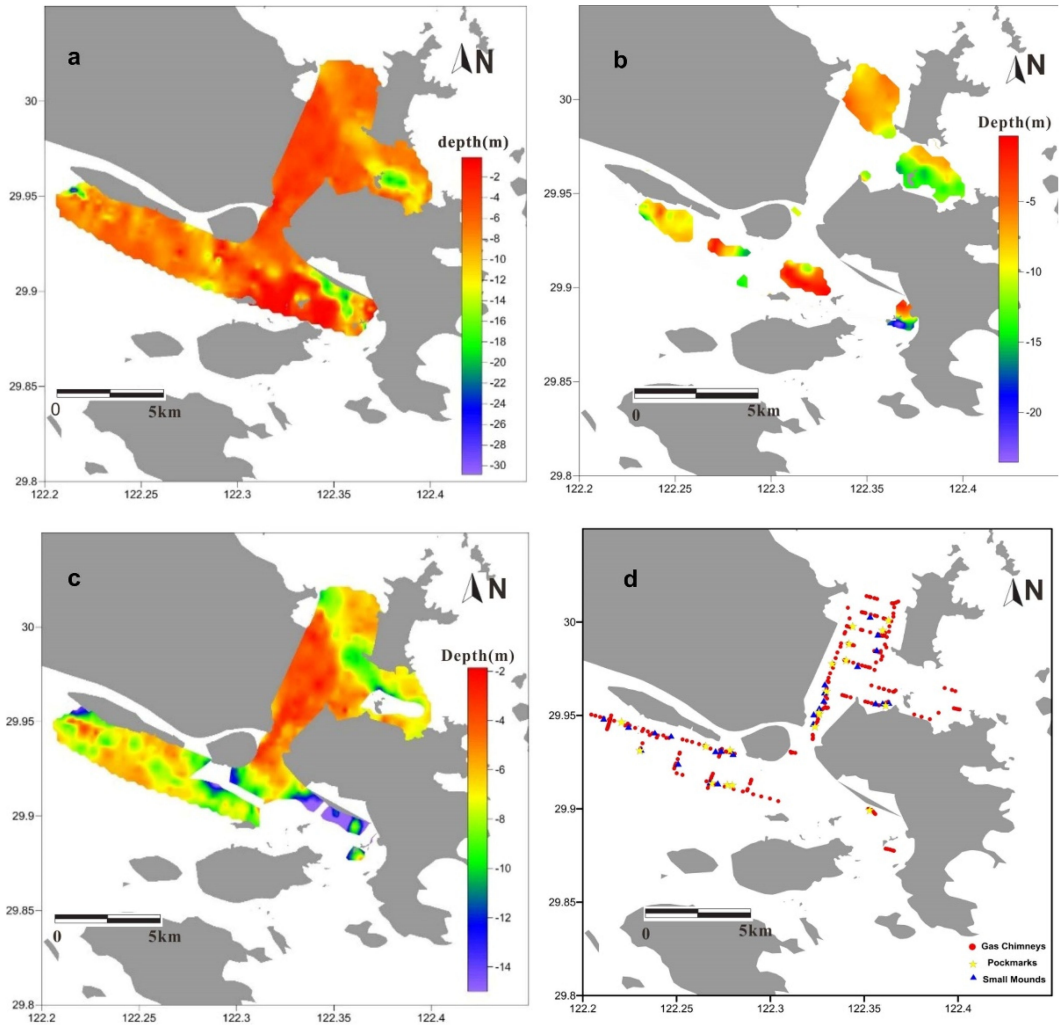

FIGURE 2
Contour maps of the identified shallow gas and strata. **(A)** Isopach map of the Holocene fine-grained clay or clayey silt strata. **(B)** Revealed burial depth of Late Pleistocene sand strata. **(C)** Burial depth of shallow gas, ranging from 2 to 15 m below the seafloor, with a mean depth of approximately 8 m. Contour maps **(A–C)** were acquired and processed using Triton Perspective software. **(D)** Distribution maps of gas chimneys, pockmarks, and small mounds. Gas chimneys are observed throughout much of the surveyed area and identified at more than 100 locations, while small mounds and pockmarks are identified at a few locations. The map was created using Surfer Golden Software 11.

The seafloor in the study area can be subdivided into two morphologic units: the tidal current scour trough and the sea-bottom plain (Figure 1C). Located on the south coast of Zhoushan Island, the terrain of the sea-bottom plain slopes down slightly from offshore to the south, with a slope of less than 3:10,000. The water depth of the plain is 15–20 m. The micro scour troughs are developed in the alongshore plain regions due to the strong tidal current scour. The tidal current scour trough is divided into the southern, middle, and the northern tidal current scour troughs. The south tidal current scour trough, located between Dengbu Island and Zhujiajian Island, extends nearly NW-SE. The maximum water depth is more than 100 m, making it the maximum water depth of the study area. The middle tidal current scour trough is located between Zhoushan Island and Zhujiajian Island, extending in a N-S direction, with water depths ranging from 14 to 20 m. The middle trough is narrow, with a width of less than 500 m at its narrowest point. The northern tidal current scour trough consists of the NWW-SEE scour tough, located between Zhoushan Island and Putuo Island, and the NNW-SSE scour tough, located between Putuo Island and Zhujiajian Island. Water depths in these channels range from 20 to 25 m, and the slope is relatively broad and gentle. The seafloor topography of the study area is characterized by significant variation in topographic relief.

The lack of borehole data in the study area limited our ability to interpret the acoustic data and understand the geological evolution. As a key part of the Changjiang subaqueous delta system, the geological information from the study area is comparable and inherited from the Changjiang subaqueous delta. Therefore, we collected two sub-bottom acoustic profiles (profile A and profile B) and four borehole data as the basis for regional stratigraphic correlation in the study area.

3.2 Holocene structure of coastal mud wedge

Based on numerous lithology and radiocarbon dating of cores and seismic profiles (Figures 3A, B), the Late Quaternary stratigraphy on the ECS inner shelf consists of Late Pleistocene terrigenous sand (fluvial and lacustrine facies) overlain by Holocene transgressive silt (Chen et al., 2000; Hori et al., 2001; Liu et al., 2007; Xu et al., 2012).

The profiles display a prominent acoustic subsurface reflector that truncates underlying strata at a water depth of 30–50 m (Figures 3A, B). Compared with previous geological and geophysical records from the Changjiang subaqueous delta (Chen et al., 2000), the Yellow River (Liu and Milliman, 2004), and the inner ECS shelf (Liu et al., 2007), this prominent acoustic reflector appears to be the base of the postglacial transgressive surface (TS), which was apparently caused by a rapid landward transgression during a rapid sea-level rise (Liu and Milliman, 2004). Below the TS tends to be a fine-sand layer indicated by cores (bottom of CH1, CJ3, Dc1, and Dc 2 in Figure 3) (Qin et al., 1987; Huang et al., 1996), presumably formed during the last low stand of sea level.

Above the TS, there are thin deposits (< 2 m), an acoustically transparent layer, which was formed during rapid sea level transgression between MWP-1A and MWP-1B (14.3–11.2 kyr BP) (Figure 3B). It should be considered a transgressive system tract (TST) (Xu et al., 2012). The transparent TST deposit becomes thinner and diminishes onshore. During this period, the Changjiang mouth retreated rapidly northwestward, and the wide southern inner shelf, being far from the Changjiang river mouth, became sediment-starved, with only a small amount of fine sediment reaching southward. Near the paleo-Changjiang mouth, however, Changjiang sediment downlapped directly onto TS due to the close proximity to the river (Figure 1A).

Above the TS or acoustically transparent thin layer, a prominent clinoform, locally 20–40 m in thickness, thins offshore to the east. Cores indicate they are dominated by muddy sediment: silty clay or clayey silt (Figure 3C). The thick package of sediment is

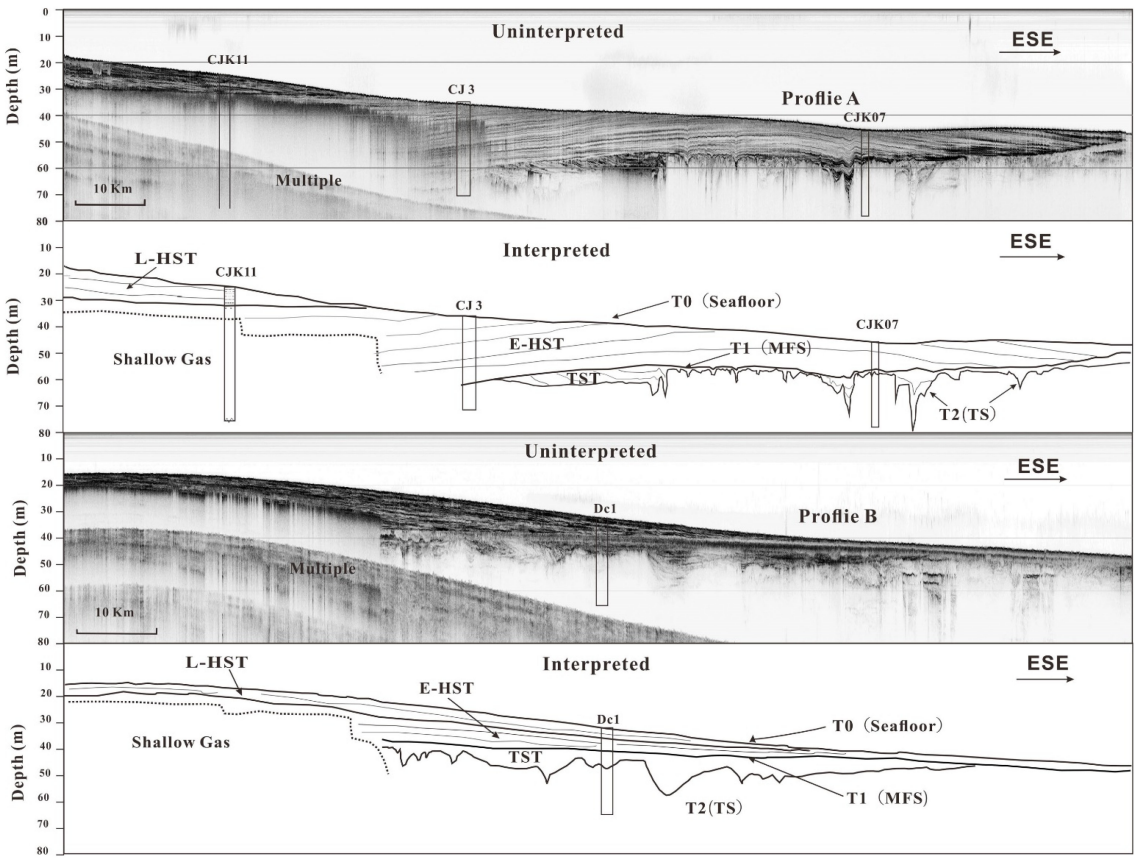

FIGURE 3
Longitudinal sub-bottom profiles in the subaqueous proximal and distal Zhe-Min coastal mud wedge. The locations of profiles and cores are shown in Figure 1A. **(A)** Profile A is located at the Changjiang subaqueous proximal mud wedge and passes through cores CJK11, CJ-3, and CJK07. Cores CJK11 and CJK07 are modified after Xu et al. (2016), and core CJ-3 is modified from Huang et al. (1996). **(B)** Profile B is located at the Changjiang subaqueous distal Zhe-Min coastal mud wedge and passes through core Dc1. Core Dc1 is modified from Qin et al. (1987). These profiles show LHST, E-HST, TST, MFS, TS, and signals of multiple reflections and biogenic shallow gas. L-HST, late highstand systems tract; E-HST, early highstand systems tract; TST, transgressive systems tract; MFS, maximum flooding surface; TS, transgressive surface. Each profile is presented in two parts: uninterpreted and interpreted. The uninterpreted profile shows the raw profile, while the interpreted profile highlights the inner reflectors in comparison with borehole cores.

termed highstand system tract (HST). It can be divided into two parts: the lower part, defined as early highstand system tract (E-HST, 8–2 kyr BP), and the upper part, defined as late highstand system tract (L-HST, 2–0 kyr BP) (Xu et al., 2012), separated either by angular unconformities (Figure 3A) or acoustically opaque strata (Figure 3B), and consisting of a prograding mud wedge.

Due to the localized high sediment supply, the Changjiang subaqueous delta might have continued to prograde during the sea level transgression from 11 to 7 kyr BP (Catuneanu, 2006). Thus, theoretically, the lower part (11–7 kyr BP) of E-HST can also be regarded as part of the TST, but it is distinctly different from the TST, which was formed during the rapid sea level transgression between MWP-1A and MWP-1B. Around 7 kyr BP, when sea level had risen to and slightly above its present level, the Changjiang mouth retreated northwestward, close to its modern location, or even farther inland. As the sea level stabilized (Chen and Stanley, 1998; Hori et al., 2001), the China Coastal Current became a more permanent feature, enabling sediments to be resuspended and transported southward. The Changjiang began to develop its mud wedge on the inner shelf of the ECS, and the southern depocenter began to receive continuous sediment inputs (Xiao et al., 2005; Xu, 2013).

4 Results

4.1 Seismic structure

Based on the truncated surfaces and the characteristics of the reflectors, three distinct acoustic units (I, II, and III, delineated as blue, yellow, and red in Figures 4–6) were identified in the sub-bottom seismic profiles.

The upper part of the seismic profiles is unit I (blue), which shows typical horizontal neritic strata characterized by the development of horizontal and/or parallel rhythmical bedding (Figures 4–6). This part of the strata covers most study area, and the thickness varies from 3 to 15 m. This is the theoretical minimum thickness due to shallow gas shielding at the bottom boundary of the Holocene strata, and the actual thickness is slightly larger (Figure 2A). The thickness in the broad terrain of the study area, including the western sea-bottom plain and the northern trough, is relatively large, normally ranging from 5 to 15 m, with an average thickness is 9 m, increasing gradually offshore (Figures 2A, 4, 5). In the middle and southern narrow trough, the thickness ranges from 2 to 8 m and is partially missing due to tidal current scour. The maximum thickness was found in the central apophysis of the southern trough, where the thickness exceeded 15 m (Figures 2A, 5, 7). Compared with the seismic profiles (Figures 3A, B), this is the Holocene fine-grained clay or clayey silt sediment of neritic facies, formed during the Holocene postglacial transgression.

Units I (blue) and II (yellow) are separated by angular unconformities, which display a prominent subsurface reflector that truncates underlying strata in profiles (Figures 3–5). This prominent truncation surface, which is uneven and erosional, suggests that this acoustic reflector belongs to the base of the postglacial transgressive surface (TS), likely caused by a rapid landward transgression during a rapid sea-level rise, as observed in the adjacent inner shelf sequences (Liu et al., 2006, 2007; Xu et al., 2012). Below the TS is unit II (yellow), characterized by inclined

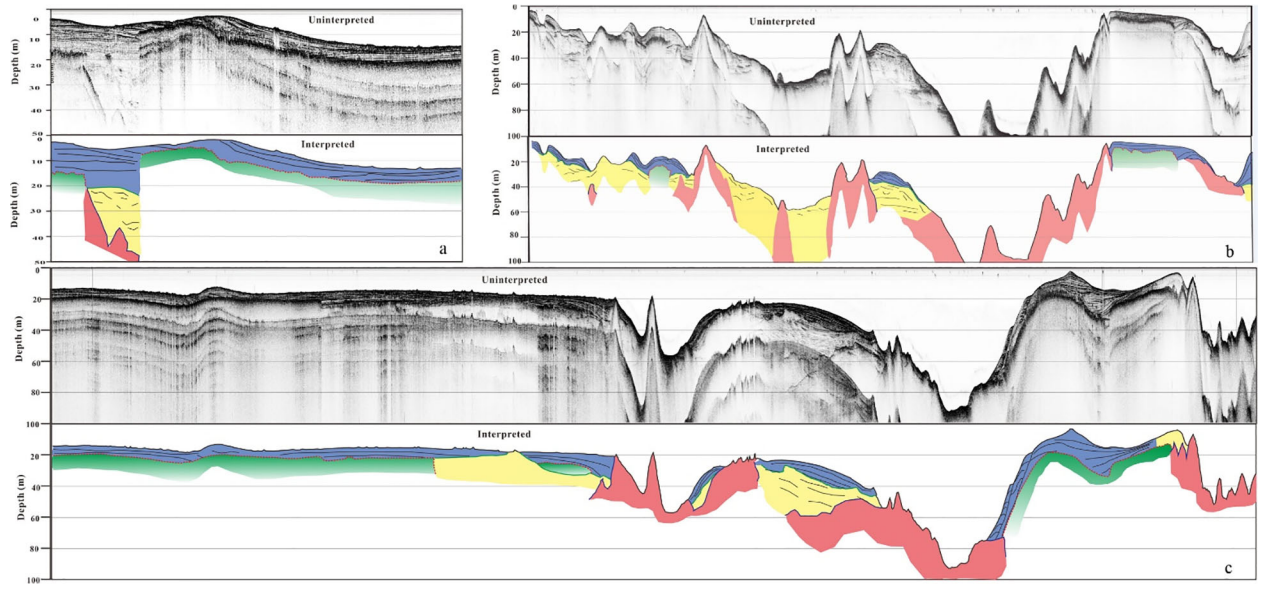

FIGURE 4
Sub-bottom profiles in the western sea-bottom plain [**(A)**, and western part of **(C)**] and southern deep scour trough [**(B)**, and eastern of **(C)**]. Units I–III are shown in blue, yellow, and red, respectively. Unit I (blue) consists of fine-grained clay or clayey silt sediments of neritic facies, formed during the Holocene post-glacial transgressive. Unit II (yellow) represents littoral facies sands or refilled channel deposits from the Late Pleistocene. Unit III (red) corresponds to the bedrock. Green highlights indicate the presence of biogenic shallow gas. The red dashed line indicates an angular unconformity separating units I (blue) and II (yellow). Refer to Figure 4 caption for definitions of sediment, color, and units. See Figure 1B for the locations of the profile.

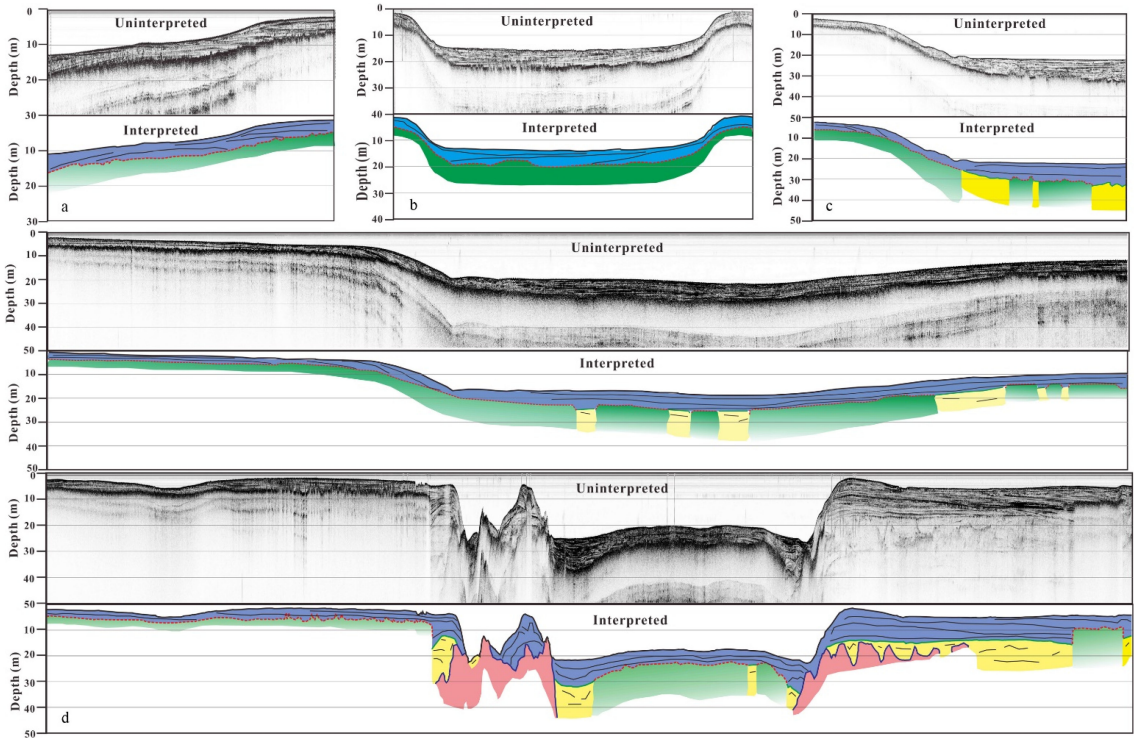

FIGURE 5
Sub-bottom profiles in the northern broad and gentle scour trough. Refer to Figure 4 caption for definitions of sediment, color, and units. See Figure 1B for the locations of the profile.

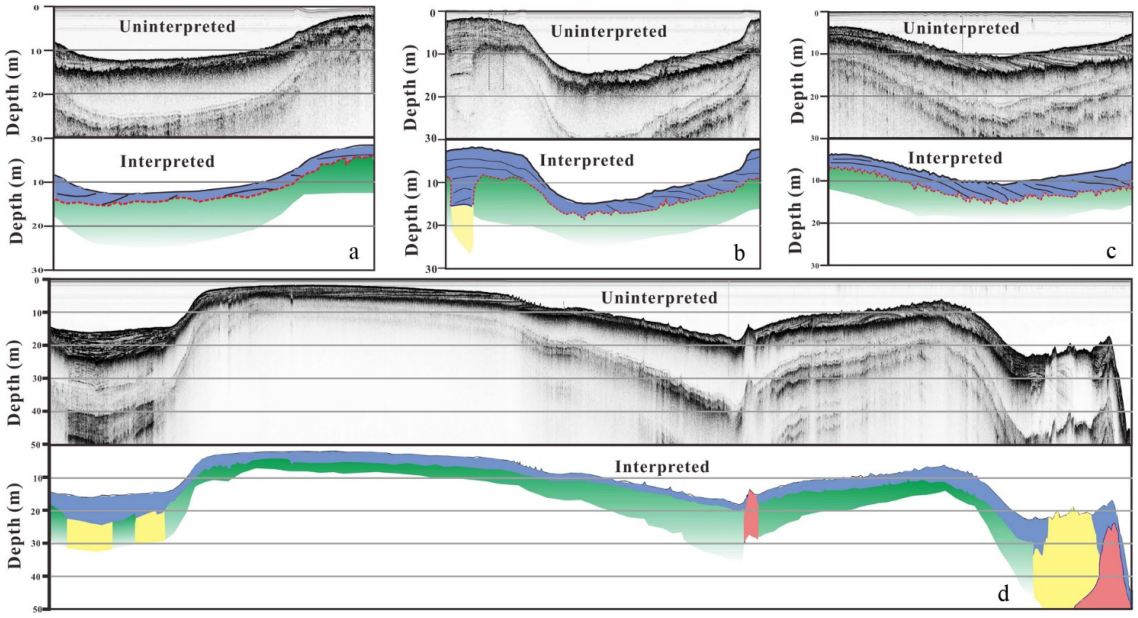

FIGURE 6
Sub-bottom profile in the middle narrow scour trough. Refer to Figure 4 caption for definitions of sediment, color, and units. See Figure 1B for the locations of the profile. Acoustic blanking and enhanced reflections are predominant in the study area and are observed across most of the surveyed areas.

bedding or cross-bedding in the seismic profiles, indicating that it consists of disorderly littoral facies sands or refilled channel deposits from the Late Pleistocene, presumably deposited or eroded during the last low stand of sea level. Since gas-charged sediment attenuates acoustic energy and limits the sub-bottom penetration, unit II is difficult to record clearly in seismic profiles and can only be observed sporadically. The thickness of unit II is greater than ~ 10 m, with the maximum thickness exceeding 30 m (Figures 2B, 4–6).

The lower part of the seismic profiles is unit III (red). The top interface shows strong reflection characteristics and can be traced to islands or reefs, with no structural signal reflection beneath, thus inferred to be underlying bedrock (Figures 2B, 4, 5E, 6). Bedrock is buried shallowly in the inner coast, with a depth of 0–30 m, and it is exposed to the seabed in the trough due to tidal current scour. A few profiles reveal that the depth of bedrock on the outer coast is more than 50 m (Figure 2B). Due to the limit of penetrability, bedrock cannot be traced in most areas. The underlying bedrock can ectend up to 100 m, even in near-bedrock island areas, as revealed by drilling on the land of a nearby island.

The lower part of the Holocene, which tends to be acoustically opaque, is marked by green. This layer indicates the presence of biogenic shallow gas (Figures 4–6). Shallow gas occurs widely in the study area (Figures 2D, 4–6), especially in the western sea-bottom plain and the northern, relatively smooth tidal current scour trough. The horizontal and vertical distribution of the shallow gas is discussed below.

4.2 Acoustic signatures of shallow gas

Based on the acoustic data for the study area, the acoustic anomalies associated with shallow gas accumulation and migration include: (1) acoustic blanking, (2) enhanced reflections, (3) gas chimneys, (4) bright spots, (5) small mounds, and (6) pockmarks (Figure 7). These acoustic anomalies provide direct evidence of the occurrence of shallow gas across the study area.

Acoustic blanking is the most dominant acoustic feature in the study area, covering over 70% of the survey lines and characterized by a complete "wipe-out" of seismic data beneath, usually occurring beneath enhanced reflections and extending laterally for up to several thousand meters (Figures 7A, B). The subsurface depths of the acoustic blanking in the study area range from about 3 m to over 15 m. Acoustic blanking is mainly observed through the Holocene muddy strata.

The acoustic blanking front is often sealed by a hatched "pavement" of bright spots, which appear as a strong reflection with higher amplitudes than the bottom reflection (Figures 7A–C).

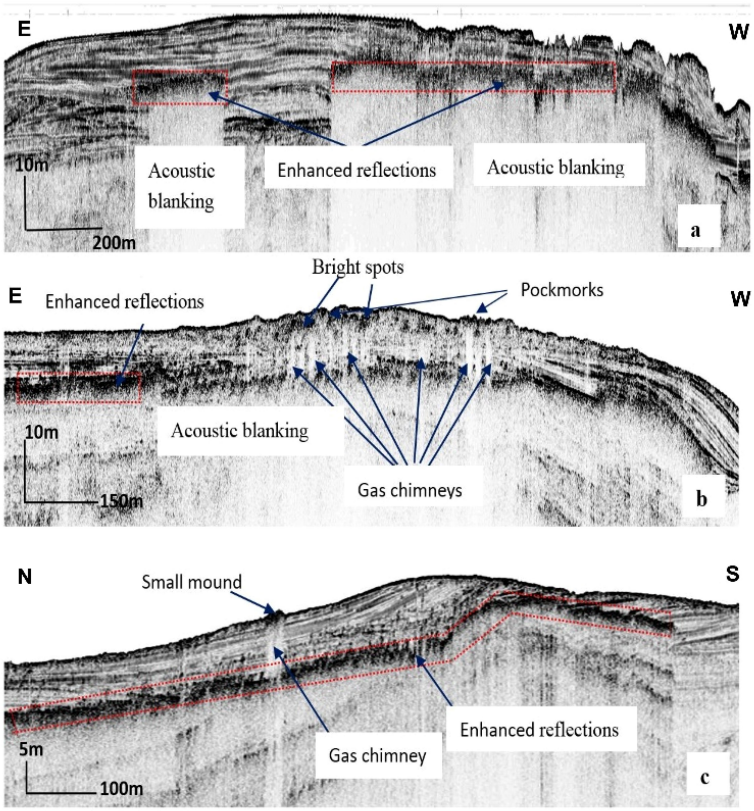

FIGURE 7
Acoustic anomalies associated with shallow gas are shown in examples of sub-bottom profiles. Refer to Figure 1B for the locations of the profile. Profiles **(A–C)** display acoustic blanking and enhanced reflections, which are predominant in the study area and observed in most of the surveyed areas. Profiles **(B, C)** reveal gas chimneys, small mounds, and pockmarks, providing evidence of shallow gas upward migration.

This enhanced reflection indicates an interface with a large acoustic impedance contrast due to the shallow gas. The enhanced reflections are laterally extensive and can reach up to 5 km. The depth of the enhanced reflections is shallower than 3–15 m below the seabed. Most of them follow the seafloor topography and are concordant with the Holocene mud strata.

Gas chimneys are observed throughout much of the surveyed area and identified at more than 100 locations (Figure 2D). Most of them are generally found in the nearshore part of the sea-bottom plain and scour trough. As an important type of acoustic anomaly associated with shallow gas, they are characterized by narrow vertical zones of acoustic blanking or attenuated seismic signals (Figure 7B). Their width ranges from 10 to 20 m and is distinguished by very bright reflections (bright spots) (Figure 7B) from their upper boundary, which is generally located less than 5 m below the seabed. Gas chimneys occur immediately above enhanced reflections, and their bottom is connected with the acoustic blanking.

Small mound features on the seafloor are observed in a few locations (Figure 7C). These mounds are less than 3 m in height and 10 m in width. The small mound structures seen in the surveyed area are associated with gas chimneys immediately below.

Most gas chimneys in the study area terminate at different fine-grained Holocene strata before reaching the seabed, with only a few cropping out and apparently creating pockmarks on the seabed (Figure 7C). Pockmarks, characterized by V-shaped incisions on the seafloor, are generally found in a few locations (Figure 7B). They appear as seabed depressions ranging from 2 to 10 m in diameter. Many pockmarks are accompanied by gas chimneys that crop out Holocene strata to the seafloor.

4.3 Distribution of shallow gas

Shallow gas is characterized by is extensive, discontinuous distribution and shallow burial in the study area (Figures 2D, 4–6). It occurs widely throughout the area (Figure 2D), especially in the western sea-bottom plain or the northern and middle troughs, where tidal current scouring is relatively weak (Dong et al., 2018). These areas extend over 10 km (Figure 2D). Shallow gas is not found in the southern deep trough or near the islands (Figure 2D). The depth of the gas front ranges from about 2 to 15 m, with an average of 7 m, indicating it is ultra-shallow gas. *The burial of shallow gas varies greatly between the lower and upper parts of the Holocene strata.* These distribution patterns suggest that the *Holocene fine* sediments are both the origin and reservoir of gas in the study area, and the Holocene fine-grain muddy sediments also serve the capping bed.

The buried depth of shallow gas in the western sea-bottom plain ranges from 4 to 12 m, with an average depth of 8 m. Some shallow gas permeates to the upper part of the Holocene fine-grain muddy silt layer (Figures 4A, C). The southern trough has the largest water depth in the study area. Due to wave washing and strong tidal current scouring (Dong et al., 2018) caused by trough narrowing, the bedrock or Pleistocene sandy sediments are exposed at the seafloor, preventing shallow gas accumulation due to the lack of muddy sediments. Only near Zhujiajian Island, where the area is weakly affected by trough narrowing, does accumulation occur, with a buried depth of 6–14 m (Figures 4B, C).

The buried depth of shallow gas ranges from 4 to 12 m in the northern broad and gentle scour trough, decreasing gradually from the middle trough to the sides (Figure 5). Sub-bottom profiles show that the buried depth of shallow gas is present in the lower part of the Holocene strata in the western area. However, shallow gas is also found in the upper part of the Holocene strata in the northern area, which is connected to the open shelf of the East China Sea and significantly affected by wave action (Figures 5D, E). Thus, fine-grained sediments are difficult to deposit, resulting in coarser Holocene deposits in the eastern compared to the western area. This weakens the sealing ability of the capping bed, allowing shallow gas to migrate to the upper part of the Holocene strata.

The minimum embedded depth occurs in the middle trough of the study area, at about 2–4 m (Figure 6). However, in contrast to the northern area, the buried depth of shallow gas increases gradually from the middle trough to the sides.

5 Discussion

5.1 Sedimentation rates and Changjiang sediment dispersal

The circulation system plays an important role in sediment transport and deposition in the Zhoushan mud area (Guo et al., 2000; Hu and Yang, 2001; Li et al., 2005). In summer, under the prevailing southeast monsoon, the northward TWC intensifies, and correspondingly, the southward ECSCC weakens, causing the rapid deposition of suspended sediments in the Yangtze Mouth. In winter, the ECSCC intensifies, carrying sediment discharge southward along the inner shelf of the ECS (Milliman et al., 1985).

The study mud area is located between the northern Changjiang delta depocenter and the southern delta distal along the Zhe-Min coast, at the edge of the junction of the Zhe-Min coastal mud wedge. The Holocene strata are widely distributed in the study area but absent in the southern deep scour trough. The thickness of the Holocene mud deposits ranges from 2 to 15 m, with most being between 5 and 10 m. The morphology and the resultant tidal currents constrain sediment deposits in this area. The maximum Holocene deposits were found in the eastern parts with bedrock shielding (Figure 2A). The Holocene deposits are generally thick in the northern and western plain areas (Figure 2A), where tidal currents are relatively weak (Dong et al., 2018). In contrast, the Holocene deposits are thin or even absent in the trough regions (Figures 5, 6), where strong tidal currents prevail (Dong et al., 2018). The long-term sedimentation rate ranged from 0.29 to 2.14 m/ka, assuming that the sediments were formed from the Middle and Late Holocene (~ 7 ka BP from Liu et al., 2006). This sedimentation rate is obviously lower than both the northern Changjiang river mouth depocenter (with a thickness if ~ 40 m over the past ~ 7 kyrs and a long-term sediment accumulation rate of 5.71 m/ka) and the southern Zhe-Min coastal depocenter (with a thickness of ~ 30 m over the past ~ 7 kyrs and a long-term sediment accumulation rate of 4.29 m/ka) (Liu et al., 2007). Given the large

area of the Zhoushan Archipelago and its proximity to the Changjiang delta and its distal mud zone, estimating the sediment accumulation rate in the study area is crucial for understanding the fate of the Changjiang sediment dispersal. However, whether the Zhoushan Archipelago is a sediment trap or sediment transport passage remains unclear due to the absence of direct measurement.

Our estimated low sediment accumulation rate in the study area, compared with the adjoined Changjiang delta and the Zhe-Min mud zone, suggests that it is a passage for sediment transport between the northern Changjiang subaqueous delta and the southward shelf region. Although suspended sediment concentration in the study area is high, the hydrodynamic conditions are enhanced by strong tidal currents and trough narrowing, which lead to active sediment resuspension and, thus, a low sedimentation rate. The low long-term sedimentation rate reveals that the study area experienced weak deposition during the Holocene. A large amount of sediment were resuspended and transported through the archipelagoes, supplying a significant volume of sediment to the Zhe-Min Coastal mud wedge.

5.2 The origin of shallow gas

The sub-bottom profiles reveal that the lower shallow gas occurs near the base of the Holocene muddy strata, and some other gas is present throughout the Holocene mud strata. The lower gassy sediments are observed in strata immediately above the Late Pleistocene/Holocene interface, related to organic matter degradation in Late Pleistocene deposits and/or Early Holocene deposits sealed by Holocene muddy strata. A substantial part of the gas apparently originates from organic matter that accumulated in sediments deposited during the Early Holocene. Acoustic blanking has been attributed to the high organic content of mud and the entrapped gas bubbles produced by the decomposition of such organic matter (Acosta, 1984; Taylor, 1992). The acoustic blanking occurs widely at the Late Pleistocene deposits/Holocene interface, suggesting that these deposits can provide good gas generation and reservoirs. The Holocene strata of the study area are fine-grained muddy deposits due to the resuspension and transportation of the Changjiang subaqueous delta (Xu et al., 2012). These fine-grained Holocene mud play a significant role in the capillary sealing ability of the capping bed, which limits or hinders the vertical migration of shallow gas from deeper layers. The large quantities of organic material and increased sediment flux are two sensitive factors that control shallow gas production in coastal sediments (Claypool and Kaplan, 1974). The environmental changes of the study area have been identified as follows since the Last Glacial Maximum: (1) floodplains associated with *groundwater discharge to the exposed shelf* during the regression period, (2) estuary and tidal flats during the transgression period, and (3) Changjiang-derived sediments deposited during the sea-level highstand. *All the above stages could have provided large quantities of organic material, thus serving as a source for gas production.* Geological studies have revealed the presence of a thin (1–2 m) peat-rich layer that can most likely be linked to the Late Pleistocene/Early Holocene formation of the inner shelf of the East China Sea (Huang et al., 1985; Liu et al., 2006). It most likely represents the widespread "basal peat" that developed on the Pleistocene surface due to the rise in groundwater level caused by the postglacial sea-level rise. This peaty layer could well be the main cause of the acoustic anomalies observed in the Lower Holocene strata in the study area (Missiaen et al., 2002). Late Pleistocene/Early Holocene gas generation was also reported in the Belgian Coast (Missiaen et al., 2002), in the Bertioga Channel, São Paulo (Félix and Mahiques, 2013), and the Patos Lagoon, southern Brazil (Weschenfelder et al., 2006). Different from most coastal environments, such as in the Black Sea (Okyar and Ediger, 1999) in the East China Sea (Ye et al., 2003), where the shallow gas was mainly formed in the Holocene sediments, it may be related to the lower sedimentation rate during the Holocene (high-stand deposits) in the study area.

Additionally, shallow gas also presents through the Middle and Upper Holocene strata. Since the sediment in the study area originated from the Changjiang River, this riverine fine-grain sediment is abundant with terrestrial and marine organic carbon from the Changjiang delta (Deng et al., 2006). Organic carbon content in sediments throughout the Holocene in the Changjiang submerged delta nearby usually > 0.5% (Wang et al., 2012; Zhan et al., 2012), which is higher than the threshold value for gas generation (Claypool and Kaplan, 1974; Rice and Claypool, 1981). The organic-rich sediments throughout the Holocene strata are also the origin of gas generation.

Moreover, the burial depth of the gas front varies greatly in the study area (Figure 2). Extremely shallow gas and the continued stretched reservoir (< 5 m burial depth) are present in the plain area or in the shallow water trough bank where high sediment accumulation is found (Figures 5, 6), while the gas front becomes deepen and patchy in the deep trough regions where strong tidal currents lead to relatively low sediment accumulation (Figures 5, 6). The constraint of sediment accumulation on shallow gas distribution was presumably related to the role of sediment accumulation in organic carbon burial and preservation, both of which are required for gas generation and accumulation in sediment (Rice and Claypool, 1981; Zhang et al., 2023).

5.3 Seabed stability and gas seepage

The sub-bottom seismic profiles show that the stratum structure of the study area consists of the Late Pleistocene coarse-grained fluvial or lacustrine facies sand strata (unit II) overlain by the Holocene fine-grained neritic facies silty clay or clayey silt strata (unit I) (Figures 4–6). The Holocene strata are widely distributed and characterized by grain size (median size of < 15 μm) (Luo et al., 2014; Xu et al., 2012), high water content (> 50%), high porosity, and low critical shear stress for erosion (τ_{cr}) (< 0.1 Pa) (Luo et al., 2014; Deng et al., 2017). These features make the sediment easily resuspended and eroded by waves and currents. Although the wave effect in the study area is weakened due to the shielding of the islands, the tidal current velocity increases obviously due to the narrowing of the islands (Jiang, 2001). Surface fine sediments are easily scoured and eroded by tidal current forces, especially in the middle and south deep troughs, where the bedrock is completely

exposed at the seabed. Shallow gas occurred widely and was characterized by extensive and continuous distribution, shallowly buried in the study area. The sub-bottom profiles show that the depth of the shallow gas front ranges from about 2 to 15 m, with an of average 7 m (Figure 2C), indicating it is the ultra-shallow gas in the shallow water area. The presence of shallow gas increases the compressibility and porosity of gas-charged sediments (Whelan et al., 1977), which suggests that the shear strength of the overlying muddy strata is decreased by the upward migration of shallow gas. The presence of ultra-shallow gas within soft muddy sediment, along with strong tidal turbulence, makes the study area vulnerable to sediment erosion.

As the representative structure of upward migration of shallow gas (Dondurur et al., 2011), gas chimneys are common and often associated with upward gas migration (Figure 2D). Gas chimneys may imply that the presence of such structures is indicative of a more permeable sediment column at the respective locations. Most gas chimneys terminate at different depths of the Holocene muddy strata before reaching the seafloor, and only a few crop out, apparently creating pockmarks or small mounds on the seafloor (Figure 7B). Although there is no evidence associated with the escaping of shallow gas from the seabed to the water in sub-bottom seismic profiles, such as acoustic plumes or cloudy turbidity (Garcia-Gil et al., 2002), gas chimneys with pockmarks or small mounds on the seafloor indicate that the shallow gas is still active (Hovland, 1989, 1990, Hovland et al., 2002, 2010; Gu et al., 2006). Most of these features are distributed in the nearshore area (Figure 2D). In these areas, the depth of water is shallow, and surface sediments are easily disturbed and resuspended. The Holocene muddy strata could not keep an efficient seal, allowing the gas to migrate upward more easily. The seepage of gas on the seafloor will substantially decrease the critical shear stress for erosion (Sun et al., 2019) and, in turn, increase the vulnerability of sediment erosion in the study area. Moreover, the erosion of surface sediment in shallow gas-bearing deposits will also accelerate the gas seepage, a process has been widely observed in the erosional submerged Changjiang Delta nearby (Chen et al., 2023). Furthermore, these areas are also the most affected areas by human activities, such as coastal engineering practices. Changes in the sedimentary environment caused by human activities affect sediment supply and transportation balance, which, in turn, influence the adjustment of sedimentary strata and make it easier for shallow gas in nearshore shallow water areas to migrate upward. This distribution characteristic suggests that strata stability is a key factor affecting upward migration and release. On the other hand, the accumulation of shallow gas poses a potential danger to the stability of marine engineering foundations. Marine engineering foundation can easily cause the release of shallow gas, potentially triggering landslides, as observed in our profiles (Figure 4C). The sharp release of high-pressure shallow gas can generate a fast flow that strongly scours seabed sediments (Ye et al., 2003). This release may also lead to uneven settlement of strata, even resulting in sunken pits (Garcia-Gil et al., 2002; Gu et al., 2006). In addition, the Late Pleistocene gas-charged coarse-grained sandy sediments are susceptible to liquefaction, which could lead to the collapse of marine engineering foundations (Ye et al., 2003). In general, shallow gas is widely distributed, still active, and easily released, coupled with an extremely unstable strata structure. The Late Pleistocene, easily liquefied, gas-charged sandy sediments are overlain by the Holocene, easily scoured muddy sediments. *Therefore, its potential impact* on seabed stability *cannot be neglected*, especially as more intensive engineering activities are planned or being implemented in the Zhoushan Archipelago to meet the increasing demands for transportation capabilities along the East China coast.

In addition to marine engineering, the adjustment of sedimentary strata would also result in the release of shallow gas. As one of the largest rivers in Asia in terms of sediment discharge (470 Mt/year), the Changjiang carried the bulk of sediment to the East China Sea. Over the past decades, damming, irrigation, and other catchment human activities in the Changjiang catchment have substantially decreased sediment loads, resulting in the erosion of the Changjiang delta (Milliman and Farnsworth, 2011; Yang et al., 2006; Yang et al., 2011; Deng et al., 2017). Compared with over 500 Mt/year before 1970 and an average of 320 Mt/year from 1993 to 2002, the sediment load at Datong decreased to about 120 Mt in recent years (Deng et al., 2017). As a result, there has been a corresponding decrease in coastal salt marsh accretion and even erosion at the subaqueous delta front. The erosion occurred mainly near the 20-m isobaths (Yang et al., 2011; Deng et al., 2017). With the construction of new dams and the South-to-North Water Diversion in the Changjiang watershed, the sediment load of the Changjiang is expected to continue to decline, and the subaqueous delta will suffer further erosion in the future. As the passage for Changjiang sediment dispersal, the risk of erosion in the Zhoushan Archipelago, including our study sites, would increase. Seafloor erosion will decrease the sealing capability of the Holocene muddy capping bed and promote the upward migration of shallow gas. However, to what extent the coastal erosion will release the buried shallow gas and lead to unpredictable consequences is worthy of our sustained attention, given the decline in Changjiang-derived sediment supply in the future.

Large river deltas and their adjoining coastal regions have long been considered important carbon sinks. Organic-rich river-fed fine-grained sediment deposits provide ideal conditions for methane-rich shallow gas generation. On the other hand, increasing human activities in the river basin and engineering practices in the coastal regions have profoundly modulated the sedimentary environment. The decreased river sediment discharge leads to sediment starvation and, in turn, erosion of delta and coastal regions. Coastal engineering adds complexity to the vulnerability of coastal regions to human activities. The evaluation of these modifications and their impacts on gas-charged sediment disturbance and the associated potential risks is still sparse and deserve extensive attention.

6 Conclusion

The strata in the study area can be classified into three geological units: Holocene fine-grained neritic facies muddy strata, Late Pleistocene coarse-grained fluvial or lacustrine facies sandy strata, and bedrock. The stratigraphy of the study area consists of Late Pleistocene littoral or fluvial facies sandy strata

that are overlain by Holocene neritic facies muddy strata. Our estimated Holocene low sediment accumulation rate (0.29~2.14 m/ka) in the study area, compared with the adjoined Changjiang delta and the Zhe-Min mud zone, suggests that it serves as a passage for sediment transport between the northern Changjiang subaqueous delta and the southward shelf region.

Seismic profiles reveal strong evidence for shallow gas accumulations in the study area, including acoustic blanking, enhanced reflections, bright spots, gas chimneys, small mounds, and pockmarks. Shallow gas is widely distributed and characterized by an extensive, continuous, and ultra-shallow burial in the study area. The shallow gas is mostly found at the Late Pleistocene/Holocene interface and within the Holocene mud strata, presumably related to organic matter degradation from the Holocene muddy strata. The Holocene muddy strata play a significant role in gas generation and the capillary sealing of gas reservoirs.

Gas chimneys have been observed at over 100 locations, indicating upward gas migration. The seepage penetrates through the seafloor and creates pockmarks or small mounds on its surface. The presence of gas chimneys with seafloor expressions, such as pockmarks or small mounds, suggests that shallow gas activity remains active. These features predominantly occur in nearshore areas, likely due to shallow water depths and significant human activities. This observation implies that strata stability is a critical factor influencing both the upward migration and release of shallow gas.

The presence of active shallow gas within thin, soft muddy strata, combined with strong tidal turbulence and human activities, indicates that the seafloor in the study area is vulnerable to sediment erosion and shallow gas seepage. This situation poses a potential threat to the stability of marine engineering foundations. The ongoing decline in Changjiang sediment discharge and the resulting erosion along the adjacent coast will inevitably lead to corresponding morphological adjustments in the study area, such as seafloor erosion. The extent to which coastal erosion may increase seepage and result in unpredictable consequences warrants our sustained attention.

Data availability statement

The raw data supporting the conclusions of this article will be made available by the authors, without undue reservation.

Author contributions

BD: Conceptualization, Data curation, Formal analysis, Funding acquisition, Investigation, Methodology, Project administration, Resources, Supervision, Validation, Visualization, Writing – original draft, Writing – review & editing. JC: Conceptualization, Data curation, Funding acquisition, Investigation, Project administration, Resources, Writing – review & editing.

Funding

The author(s) declare financial support was received for the research, authorship, and/or publication of this article. This study was supported by the Innovation Program of the Shanghai Municipal Education Commission (2021-01-07-00-08-E00102) and the National Natural Science Foundation of China (42476164). The authors appreciate the assistance of Ruifeng Fang and the crew members of the research vessel RungJiang for chirp data acquisition during a public cruise funded by the National Science Foundation of China.

Acknowledgments

We are grateful for the comments and advice from Prof. Shilun Yang.

Conflict of interest

The authors declare that the research was conducted in the absence of any commercial or financial relationships that could be construed as a potential conflict of interest.

Generative AI statement

The author(s) declare that no Generative AI was used in the creation of this manuscript.

Publisher's note

References

Acosta, J. (1984). Occurrence of acoustic masking in sediments in two areas of the continental shelf of Spain: Ría de Muros-Noia (NW) and Gulf of Cádiz (SW). *Mar. Geology* 58, 427–434. doi: 10.1016/0025-3227(84)90212-3

Allision, M. A., Dellapanna, T. M., Gordon, E. S., Mitra, S., and Petsch, S. T. (2010). Impact of Hurricane Katrina (2005) on shelf organic carbon burial and deltaic evolution. *Geophysical Res. Letters.* 37, 193–195. doi: 10.1029/2010GL044547

Catuneanu, O. (2006). *Principles of sequence stratigraphy* (Amsterdam: Elsevier Press), 386.

Chen, Y. F., Deng, B., Zhang, G. L., Zhang, W. G., and Gao, S. (2023). Response of shallow gas-charged holocene deposits in the yangtze delta to meter-scale erosion induced by diminished sediment supply: increasing greenhouse gas emissions. *J. Geophysical Research: Earth Surface* 128, e2022JF006631. doi: 10.1029/2022JF006631

Chen, Z. Y., Saito, Y., Kanai, Y., Wei, T. Y., and Li., L. (2004). Low concentration of heavy metals in the Yangtze estuarine sediments, China: a diluting setting. *Estuar. Coast. And Shelf Sci.* 60, 91–100. doi: 10.1016/j.ecss.2003.11.021

Chen, Z. Y., Song, B. P., Wang, Z. H., and Cai, Y. L. (2000). Late Quaternary evolution of the subaqueous Yangtze Delta, China: Sedimentation, stratigraphy, palynology, and deformation. *Mar. Geology* 162, 423–441. doi: 10.1016/S0025-3227(99)00064-X

Chen, Z. Y., and Stanley, D. J. (1998). Sea-Level Rise on Eastern China's Yangtze Delta. *J. Coast. Res.* 14, 360–366.

Claypool, G. E., and Kaplan, I. (1974). *The origin and distribution of methane in marine sediments, Natural gases in marine sediments* (Boston: Springer), 99–139.

Cukur, D., Krastel, S., Tomonaga, Y., Çağatay, M. N., and Meydan, A. F. (2013). Seismic evidence of shallow gas from lake van, eastern Turkey. *Mar. Petroleum Geology.* 48, 341–353. doi: 10.1016/j.marpetgeo.2013.08.017

Davis, A. M. (1992). Shallow gas: an overview. *Cont. Shelf Res.* 12, 1077–1079. doi: 10.1016/0278-4343(92)90069-V

Deng, B., Wu, H., Yang, S. L., and Zhang, J. (2017). Longshore suspended sediment transport and its implications for submarine erion off the Yangtze River Estuary. *Esturine Coast. Shelf Sci.* 190, 1–10. doi: 10.1016/j.ecss.2017.03.015

Deng, B., Zhang, J., and Wu, Y. (2006). Recent sediment accumulation and carbon burial in the East China Sea. *Global Biogeochemical Cycles* 20, GB3014. doi: 10.1029/2005GB002559

Dondurur, D., Çifçi, G., Drahor, M. G., and Coşkun, S. (2011). Acoustic evidence of shallow gas accumulations and active pockmarks in the?zmir gulf, aegean sea. *Mar. Petroleum Geology.* 28, 1505–1516. doi: 10.1016/j.marpetgeo.2011.05.001

Dong, C., Chen, J. B., Xie, Y. Q., Wang, J. Q., and Chen, X. B. (2018). Transportation of suspended sediment in Shenjiamen offshore area of Zhoushan. *Mar. Geology Quaternary Geology.* 38, 78–86.

Duan, Z. H., and Mao, S. D. (2006). A thermodynamic model for calculating methane solubility, density and gas phase composition of methane-bearing aqueous fluids from 273 to 523 K and from 1 to 2000 bar. *Geochim. Cosmochim. Acta* 70, 3369–3386. doi: 10.1016/j.gca.2006.03.018

Emeis, K. C., Brüchert, V., Currie, B., Endler, R., Ferdelman, T., Kiessling, A., et al. (2004). Shallow gas in shelf sediments of the Namibian coastal upwelling ecosystem. *Continental Shelf Res.* 24, 627–642. doi: 10.1016/j.csr.2004.01.007

Félix, C. A., and Mahiques, M. M. (2013). *Late quaternary evolution and shallow gas formation in a tropical estuarine environment: the case of the Bertioga channel, Brazil.* IEEE/OES Acoustics in Underwater Geosciences Symposium, Rio de Janeiro, Brazil. doi: 10.1109/RIOAcoustics.2013.6684003

Gao, S. (2010). Changjiang delta sedimentation in response to catchment discharge changes: Progress and problems. *Adv. Earth Science.* 25, 233–241.

Garcia-Gil, S., Vilas, F., and Garcia-Garcia, A. (2002). Shallow gas features in incised-valley fills (Ría de Vigo, NW Spain): a case study. *Continental Shelf Res.* 22, 2303–2315. doi: 10.1016/S0278-4343(02)00057-2

Gu, Z. F., Zhan, Z. X., and Liu, H. S. (2006). Seismic features of shallow gas in the western area of the Yellow Sea. *Mar. geology quaternary geology.* 26, 65–74.

Guan, B. X. (1982). "An overview of the current system of the East China Sea," in *The Geology of Yellow Sea and East China Sea* (Beijing: Science Press), 126–133.

Guo, Z. G., Yang, Z. S., Qu, Y. H., and Fan, D. J. (2000). Study on comparison sedimentary geochemistry of mud areas on the East China Sea continental shelf. *Acta Sedimentologica Sinica.* 18, 284–289.

Hori, K., Saito, Y., Zhao, Q., Cheng, X., and Wang, P. (2001). Sedimentary facies and Holocene progradation rates of the Changjiang (Yangtze) delta, China. *Geomorphology* 41, 233–248. doi: 10.1016/S0169-555X(01)00119-2

Hovland, M. (1989). The formation of pockmarks and their potential influence on offshore construction. *Q. J. Eng. Geology Hydrology.* 22, 131–138. doi: 10.1144/GSL.QJEG.1989.022.02.04

Hovland, M. (1990). Suspected gas-associated clay diapirism on the seabed off Mid Norway. *Mar. Petroleum Geology.* 7, 267–276. doi: 10.1016/0264-8172(90)90004-Z

Hovland, M., Gardner, J. V., and Judd, A. G. (2002). The significance of pockmarks to understanding fluid flow processes and geohazards. *Geofluids.* 2, 127–136. doi: 10.1046/j.1468-8123.2002.00028.x

Hovland, M., Heggland, R., De Vries, M. H., and Tjelta, T. I. (2010). Unitepockmarks and their potential significance for predicting fluid flow. *Mar. Petroleum Geology.* 27, 1190–1199. doi: 10.1016/j.marpetgeo.2010.02.005

Hu, R. J., Wu, J. Z., Zhu, L. H., and Fang, M. F. (2009). Characteristic of surface sediment transport in Zhoushan archipelago sea area, East China Sea. *Periodical Ocean Univ. China.* 39, 495–500.

Hu, D. X., and Yang, Z. S. (2001). *The Key Process of Marine Fluxes in East China Sea* (Beijing: China Ocean Press), 3–13.

Huang, H. Z., Shen, B. P., and Hu, Q. S. (1985). Geological implication of geophysical data in Holocene Changjiang subaqueous delta. *Mar. Geology Quaternary Geology.* 5, 87–100.

Huang, H. Z., Tang, B. G., and Yang, W. D. (1996). *Sedimentological Geology in the Yangtze River Delta Area*. Beijing, China: Geology Publishing Company). 242 pp.

Hustoft, S., Bünz, S., and Mienert, J. (2010). Three-dimensional seismic analysis of the morphology and spatial distribution of chimneys beneath the Nyegga pockmark field, offshore mid-Norway. *Basin Res.* 22, 465–480. doi: 10.1111/j.1365-2117.2010.00486.x

Jiang, G. J. (2001). The characteristics of hydro-dynamics and sediments in the strait channels of Zhoushan Islands area. *J. Zhejiang Univ.* 28, 82–91.

Judd, A. G., and Hovland, M. (1992). The evidence of shallow gas in marine sediments. *Continental Shelf Res.* 12, 1081–1096. doi: 10.1016/0278-4343(92)90070-Z

Judd, A. G., and Hovland, M. (2007). *Submarine Fluid Flow, the Impact on Geology, Biology, and the Marine Environment* (Cambridge: Cambridge University Press), 475pp.

Lazar, M., Schattner, U., and Reshef, M. (2012). The great escape: An intra-Messinian gas system in the eastern Mediterranean. *Geophysical Res. Letters.* 39, 20309. doi: 10.1029/2012GL053484

Lee, H. J., and Chao, S. Y. (2003). A climatological description of circulation in and around the East China Sea. *Deep Sea Res. Part II Topical Stud. Oceanography.* 50, 1065–1084. doi: 10.1016/S0967-0645(03)00010-9

Li, G. X., Yang, Z. G., and Liu, Y. (2005). *Study on Sedimentary Environment in East China Sea* (Beijing: Science Press), 33–44.

Lin, C. M., Li, Y. L., Zhuo, H. C., Shurr, G. W., Ridgley, J. L., Zhang, Z. P., et al. (2010). Features and sealing mechanism of shallow biogenic gas in incised valley fills (the Qiantang River, eastern China): A case study. *Mar. Petroleum Geology* 27, 909–922. doi: 10.1016/j.marpetgeo.2009.11.006

Lin, C., Zhang, X., Xu, Z., Deng, C., and Yin, Y. (2015). Sedimentary characteristics and accumulation conditions of shallow-biogenic gas for the late quaternary sediments in the changjiang river delta area. *Adv. Earth Science.* 30, 589–601.

Liu, J. P., Li, A. C., Xu, K. H., Velozzi, D. M., and Yang, Z. S. (2006). Sedimentary features of the Yangtze River-derived along-shelf clinoform deposit in the East China Sea. *Continental Shelf Res.* 26, 2141–2156. doi: 10.1016/j.csr.2006.07.013

Liu, J. P., and Milliman, J. D. (2004). Reconsidering melt-water pulses 1A and 1B: Global impacts of rapid sea-level rise. *J. Ocean Univ. China.* 3, 183–190. doi: 10.1007/s11802-004-0033-8

Liu, J. P., Xu, K. H., Li, A. C., Milliman, J. D., and Velozzi, D. M. (2007). Flux and fate of Yangtze River sediment delivered to the East China Sea. *Geomorphology.* 85, 208–224. doi: 10.1016/j.geomorph.2006.03.023

Luo, G. F., Deng, B., and Yang, S. L. (2014). A Preliminary Study of the High Resolution Sub-bottom Stratigraphic Structures and Sedimentary Features in the Mud Area along Southern Distal Yangtze Subaqueous Delta: An example from the area off eastern Zhujiajian island. *Acta Sedimentologica Sinica.* 32, 296–305.

Mazumdar, A., Peketi, A., Dewangan, P., Badesab, F., Ramprasad, T., Ramana, M. V., et al. (2009). Shallow gas charged sediments off the Indian west coast: genesis and distribution. *Mar. Geology.* 267, 71–85. doi: 10.1016/j.margeo.2009.09.005

Milliman, J. D., and Farnsworth, K. L. (2011). *River Discharge to the Coastal Ocean: Run-off, erosion, and delivery to the coastal ocean* (Cambridge: Cambridge University Press), 1–10.

Milliman, J. D., Shen, H. T., Yang, Z. S., and Meade, R. H. (1985). Transport and deposition of river sediments in the Changjiang estuary and adjacent continental shelf. *Cont. Shelf Res.* 4, 37–45. doi: 10.1016/0278-4343(85)90020-2

Missiaen, T., Murphy, S., Loncke, L., and Henriet, J. P. (2002). Very high-resolution seismic mapping of shallow gas in the Belgian coastal zone. *Continental Shelf Res.* 22, 2291–2301. doi: 10.1016/S0278-4343(02)00056-0

Okyar, M., and Ediger, V. (1999). Seismic evidence of shallow gas in the sediment on the shelf off Trabzon, southeastern Black Sea. *Continental Shelf Research* 19, 575–587. doi: 10.1016/S0278-4343(98)00111-3

Orange, D., Garcia-Garcia, A., Lorenson, T., Nittrouer, C., Milligan, T., Miserocchi, S., et al. (2005). Shallow gas and flood deposition on the po delta. *Mar. Geology.* 222, 159–177. doi: 10.1016/j.margeo.2005.06.040

Qin, Y. S., Zhao, Y. Y., and Chen, L. R. (1987). *Geology of East China Sea* (Beijing: Science Press), 1–91.

Qin, Y. S., and Zheng, T. M. (1982). *A Study of Distribution Pattern of Sediments on the Continental Shelf of the East China Sea: The Geology of Yellow Sea and East China Sea* (Beijing: Science Press), 39–51.

Reeburgh, W. S. (2007). Oceanic methane biogeochemistry. *Chem. Rev.* 107, 486–513. doi: 10.1021/cr050362v

Rice, D. D., and Claypool, G. E. (1981). Generation, accumulation, and resource potential of biogenic gas. *Am. Assoc. Petroleum Geologists Bull.* 65, 5–25. doi: 10.1306/2F919765-16CE-11D7-8645000102C1865D

Schatter, U., Lazar, M., Harari, D., and Waldmann, N. (2012). Active gas migration systems offshore northern Israel, first evidence from seafloor and subsurface data. *Continental Shelf Res.* 48, 167–172. doi: 10.1016/j.csr.2012.08.003

Scott, A. R., Kaiser, W. R., and Ayers, W. B. (1994). Thermogenic and secondary biogenic gases, San Juan Basin, Colorado and New Mexico: Implications for coalbed gas producibility. *AAPG Bull.* 78, 1186–1209. doi: 10.1306/A25FEAA9-171B-11D7-8645000102C1865D

Shepard, F. P., Emery, K. O., and Gould, H. R. (1949). *Distribution of sediments on East Asiatic continental shelf* (State of California: University of Southern California Press), 64.

Sun, H., Chen, Z., Lai, X., Yan, X., and Hu, T. (2019). Influence of shallow gas on the geotechnical properties of pockmark soil: A case study in the East China Sea. *Appl. Ocean Res.* 93, 101966. doi: 10.1016/j.apor.2019.101966

Sun, Q. L., Wu, S. G., Cartwright, J., and Dong, D. D. (2012). Shallow gas and focused fluid flow systems in the Pearl River Mouth Basin, northern South China Sea. *Mar. Geology.* 315–318, 1–14. doi: 10.1016/j.margeo.2012.05.003

Taylor, D. I. (1992). Nearshore shallow gas around the U.K. *Coast. Continental Shelf Res.* 12, 1135–1144. doi: 10.1016/0278-4343(92)90074-T

Wang, A. J., Gao, S., and Yang, Y. (2004). Sediment distribution and shape characteristics of gravel beaches, Zhujiajian island, Zhejiang province. *J. Nanjing University: Natural Science.* 40, 747–759.

Wang, X., Shi, X. F., Wang, G. Q., Qiao, S. Q., Wang, K. S., and Yao, Z. Q. (2015). Late Quaternary sedimentary environmental evolution offshore of the Hangzhou Bay, East China—implications for sea level change and formation of Changjiang alongshore current. *Chin. J. Oceanology Limnology.* 33, 748–763. doi: 10.1007/s00343-015-4172-0

Wang, M., Zheng, H., Yang, S., and Fan, D. (2012). Environmental information in subaqueous yangtze river delta since holocene. *J. Tongji Univ. (Natural Science)* 40, 473–477.

Weschenfelder, J., Corrêa, I. C., Aliotta, S., Pereira, C. M., and Vasconcelos, V. E. (2006). Shallow gas accumulation in sediments of the Patos Lagoon, southern Brazil. *Anais Da Academia Bras. Ciências.* 78, 607–614. doi: 10.1590/S0001-37652006000300017

Whelan, T., Colemen, J. M., Suhayda, J. N., and Roberts, H. H. (1977). Acoustical penetration and shear strength in gas-charged sediment. *Mar. Geotechnology.* 12, 147–159. doi: 10.1080/10641197709379776

Wilkens, R. H., and Richardson, M. D. (1998). The influence of gas bubbles on sediment acoustic properties: *in situ*, laboratory, and theoretical results from Eckernförde Bay, Baltic Sea. *Continental Shelf Res.* 18, 1859–1892. doi: 10.1016/S0278-4343(98)00061-2

Xia, X. M., Yang, H., Li, Y., and Li, B. G. (2004). Modern sedimentation rates in the contiguous sea area of changjiang estuary and Hangzhou bay. *Acta sedimentologica sinica.* 22, 130–135.

Xiao, S. B., Li, A. C., and Chen, M. H. (2005). Recent 8ka mud records of the East Asian Winter Monsoon from the Inner Shelf of the East China Sea. *Earth Science.* 30, 573–581.

Xu, T. Y. (2013). *The study of high resolution sequence stratigraphy of Holocene in the Yangtze River delta area* (Beijing: University of Chinese Academy of Science).

Xu, K. H., Li, A. C., Liu, J. P., Milliman, J. D., Yang, Z. S., Liu, C. S., et al. (2012). Provenance, structure, and formation of the mud wedge along inner continental shelf of the East China Sea: A synthesis of the Yangtze dispersal system. *Mar. Geology.* 291-294, 176–191. doi: 10.1016/j.margeo.2011.06.003

Xu, T. Y., Wang, G., Shi, X., Wang, X., Yao, Z., Yang, G., et al. (2016). Sequence stratigraphy of the subaqueous Changjiang (Yangtze River) delta since the Last Glacial Maximum. *Sedimentary Geology.* 331, 132–147. doi: 10.1016/j.sedgeo.2015.10.014

Yang, Z. S., and Chen, X. H. (2007). Centurial high resolution records of sediment grain-size variation in the mud area of the Changjiang (Yangtze River) Estuary and its influencial factors. *Quaternary Sci.* 27, 690–699.

Yang, S. L., Li, M., Dai, S. B., Liu, Z., and Zhang, J. (2006). Drastic decrease in sediment supply from the Yangtze River and its challenge to coastal wetland management. *Geophysical Res. Letters.* 33, 272–288. doi: 10.1029/2005GL025507

Yang, S. L., Milliman, J. D., and Li, P. (2011). 50 000 dams later: Erosion of the Yangtze River and its delta. *Global Planetary Change* 75, 14–20. doi: 10.1016/j.gloplacha.2010.09.006

Yang, S. L., Shi, Z., Zhao, H. Y., Li, P., and Dai, S. B. (2004). Research Note: Effects of human activities on the Yangtze River suspended sediment flux into the estuary in the last century. *Hydrol. Earth Syst. Sci.* 8, 1210–1216. doi: 10.5194/hess-8-1210-2004

Ye, Y. C., Chen, J. R., and Pan, G. F. (2003). A study of formation cause, existing characteristics of the shallow gas and its danger to engineering. *Donghai Mar. Science.* 21, 27–36.

Zhan, Q., Wang, Z., Xie, Y., Xie, J., and He, Z. (2012). Assessing C/N and δ13C as indicators of Holocene sea level and freshwater discharge changes in the subaqueous Yangtze delta, China. *Holocene* 22, 697–704. doi: 10.1177/0959683611423685

Zhang, X., Deng, B., Chen, Y. Y., Chen, Y. F., Wang, Z. H., and Wu, J. X. (2023). Shallow gas in Holocene sediments of the Pearl River Estuary and the implication for anthropogenic effects on its release. *Global Planetary Change* 220, 103999. doi: 10.1016/j.gloplacha.2022.103999

Zheng, M. H., Jiang, S. M., and Xing, F. (2011). *Quantitative analysis on evolution of erosion and deposition in Nanhui tidal flat of Yangtze estuary*. 2011 International Conference on Electric Information and Control Engineering (ICEICE), Wuhan. 3450–3453. doi: 10.1109/ICEICE.2011.5777917

Zhou, L. C., Li, J., Gao, J. H., Bai, F. L., and Zhao, J. T. (2009). Comparison of core sediment grain-size characteristics between Yangtze River estuary and Zhoushan islands and its significance to sediment analysis. *Mar. Geology Quaternary Geology.* 29, 21–27.

Zhou, Y. K., Yan, C. H., and Li, X. Q. (2016). The spatial distribution characteristics of shallow gas in soft soil layer of Quaternary Holocene and its effect on geological hazard. *Geotechnical Invest. Surveying* 44, 17–20.